Journal of Integrative Neuroscience

J. Integr. Neurosci. **2026**; 25(3): 47039
https://doi.org/10.31083/JIN47039

Original Research

Microglial Lipid Droplet Accumulation: A Pathological Nexus Between Obesity and Depression

Xijin Liu[1,†], Jiacheng Chen[2,†], Yangzhi Xie[1], Ping Zhang[1], Zhengyang Yuan[1], Yili Yi[1], Zhao Pan[1,*]

[1]Department of Neurology, The Affiliated Nanhua Hospital, Hengyang Medical School, University of South China, 421001 Hengyang, Hunan, China
[2]Department of Intensive Care Unit, The Affiliated Nanhua Hospital, Hengyang Medical School, University of South China, 421001 Hengyang, Hunan, China
*Correspondence: pzxnwh@163.com (Zhao Pan)
[†]These authors contributed equally.

Academic Editors: Woo-Yang Kim and Bettina Platt
Submitted: 29 September 2025 Revised: 30 December 2025 Accepted: 16 January 2026 Published: 16 March 2026

Abstract

Background: A high-fat diet (HFD) has been implicated in the induction of depressive-like behaviors, yet the underlying mechanisms remain incompletely elucidated. Growing evidence indicates that microglia-mediated neuroinflammation plays a critical role in the pathogenesis of depression, with excessive lipid droplet (LD) accumulation emerging as an early trigger for neuroinflammatory cascades. The aim of this study was to investigate microglial LD accumulation and the associated neuroinflammatory response in a model of HFD-induced depression. **Methods**: Diet-induced obese (DIO) mice were compared with normal control (Con) mice. Depressive-like behaviors were evaluated through a battery of behavioral tests. Hippocampal neuronal damage and microglial activation were assessed using histological and immunofluorescence techniques. A co-culture system of glial cell-enriched isolates and hippocampal neurons was employed to evaluate the neurotoxic potential of DIO microglia. LD accumulation in microglia was quantified *in vivo* and *in vitro* using Bodipy staining, Oil Red O staining, and electron microscopy. Untargeted lipidomics was performed on glial cells to characterize alterations in lipid metabolism. **Results**: Compared with Con mice, DIO mice exhibited significant depressive-like behaviors and hippocampal neuronal damage, accompanied by enhanced microglia-mediated neuroinflammation. In the co-culture system, microglia from DIO mice demonstrated increased neurotoxicity toward hippocampal neurons. Bodipy staining and electron microscopy revealed increased accumulation of LDs in the hippocampal microglia of DIO mice. This was further confirmed in glial cells *in vitro*. Lipidomic profiling identified substantial disturbances in lipid metabolism in DIO microglia. **Conclusion**: Diet-induced obesity leads to depressive-like behaviors and hippocampal neuronal damage, which is associated with microglia-mediated neuroinflammation and intracellular accumulation of LDs. The enhanced neurotoxicity of DIO microglia, coupled with pronounced lipid metabolic dysregulation, suggests that lipid-laden microglia may contribute to the link between obesity and depression via neuroinflammatory mechanisms.

Keywords: depression disorder; obesity; lipid droplet; neuroinflammation diseases; microglia

1. Introduction

Major depressive disorder is one of the most prevalent psychiatric disorders globally, contributing significantly to disability and diminished quality of life. While its etiology is not fully understood, depression is increasingly recognized as a multifactorial condition influenced by genetic, environmental, and metabolic interactions [1]. Notably, the global increase in consumption of high-fat diets (HFD) has been strongly linked to an increased risk of depressive symptoms, although the underlying neurobiological mechanisms remain poorly defined [2]. This knowledge gap hinders the development of effective interventions for diet-associated mood disorders. Emerging evidence suggests that HFD-induced systemic inflammation can disrupt the integrity of the blood-brain barrier and promote microglial activation, thereby facilitating neuroinflammation [3]. A central mechanistic hypothesis posits that neuroinflammation, a state of heightened and sustained immune activation in the brain, serves as a key mediator linking nutritional imbalance to emotional dysfunction [4]. Microglia, the resident immune cells of the central nervous system, play a central role in this process. Under physiological conditions, microglia support neuronal health through constant surveillance and synaptic maintenance. However, under metabolic stress induced by HFD, they can shift toward a pro-inflammatory phenotype, releasing cytokines and chemokines that negatively impact neuronal function and viability [5]. Recent groundbreaking studies have demonstrated that intracellular accumulation of lipid droplets in microglia is a critical early event in the initiation and persistence of neuroinflammation [6,7]. This phenomenon, increasingly termed “microglial lipidosis”, does not merely represent passive lipid storage but is also an indicator of active cellular transformation with functional consequences. Lipid-laden microglia display enhanced release of inflammatory mediators, impaired phagocytic capacity, and diminished synaptic support [8,9].

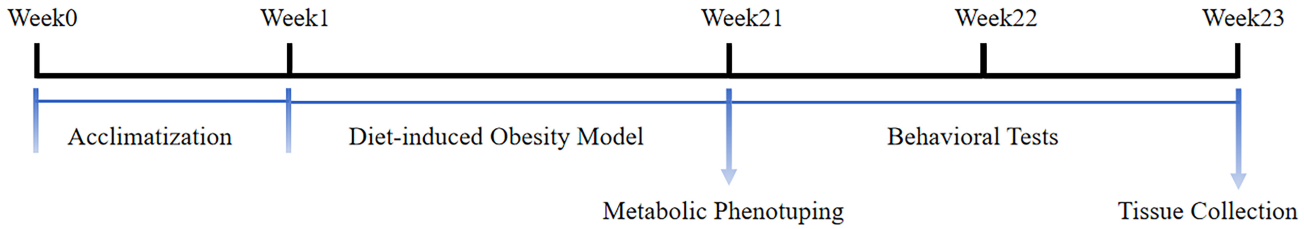

Fig. 1. Experimental design and timeline. Mice were fed a control or high-fat diet (HFD) for 20 weeks, followed by behavioral tests (Open Field Test, Sucrose Preference Test, Tail Suspension Test, Forced Swim Test). Hippocampal tissues were then collected for histological, biochemical, and lipidomic analyses.

The hippocampus, a brain region critical for mood regulation and cognitive function, appears particularly susceptible to these diet-induced changes [10,11]. Although the link between systemic inflammation and depression is well established, the role of microglial lipid accumulation as a central mechanism in HFD-induced depression remains poorly understood. The lipidomic profiles of microglia under dietary stress have yet to be fully characterized. Moreover, it is not yet known how their altered metabolism directly contributes to neuronal dysfunction *in vivo* and *in vitro*.

The aim of this work was to investigate a potential mechanistic connection between the accumulation of microglial lipid droplets (LDs) and the onset of depression, thereby offering a novel perspective on how dietary fats may influence brain immunity and emotional health. These findings may ultimately reveal new therapeutic strategies for targeting immunometabolic pathways in the treatment of depression.

2. Methods

2.1 Animal and Grouping

Male C57BL/6J mice (6-week-old) were purchased from Gempharmatech (Nanjing, Jiangsu, China), and maintained under standard housing conditions (12-h light/dark cycle, 22 ± 1 °C, 50–60% humidity) with ad libitum access to food and water. The use of male mice in this initial study was to control for potential confounding associated with hormonal fluctuations during the female estrous cycle. After a one-week acclimatization period, the mice were randomly assigned to two experimental groups. The control group (Con) was fed a standard chow diet (10% of kcal from fat), while the diet-induced obese (DIO) group was maintained on an HFD (D12492). The fat in the D12492 diet is provided primarily by lard and soybean oil. This formulation was established to reliably induce obesity and metabolic syndrome, with 60% of kcal derived from fat (Research Diets, New Brunswick, NJ, USA; catalog No. D12492). Mice were fed D12492 for 20 weeks to induce obesity and depressive-like phenotypes. This period extended beyond the typical duration for induction of weight gain (8–12 weeks), ensuring the development of chronic metabolic dysfunction and stable, robust depressive-like behaviors associated with sustained neuroinflammation and microglial activation, as previously described [12,13]. Body weight and food intake were recorded weekly throughout the experimental period. Following the dietary intervention, a series of behavioral tests were conducted sequentially to assess depressive-like behaviors, including the sucrose preference test, tail suspension test, and forced swim test. Upon the completion of behavioral assessments, all mice were deeply anesthetized with sodium pentobarbital (50 mg/kg, i.p.; cat. no. P3761, Sigma-Aldrich, St. Louis, MO, USA). The depth of anesthesia was confirmed by the absence of response to a toe-pinch reflex. Subsequently, mice were transcardially perfused with phosphate-buffered saline (PBS) while under deep anesthesia. Brain tissues were promptly harvested and processed for subsequent histological, biochemical, and lipidomic analyses. The hippocampus regions were microdissected for glial cell culture, or immediately frozen in liquid nitrogen and stored at –80 °C for further analysis (Fig. 1). The cell line has been validated by short tandem repeat authentication and surface marker analysis. Mycoplasma Contamination Testing was performed using a polymerase chain reaction (PCR)-based mycoplasma detection kit. The tests yielded negative results both at the beginning and at the end of the experimental period, confirming the absence of mycoplasma contamination.

2.2 Assessment of Metabolic Phenotype

To comprehensively evaluate the systemic metabolic phenotype of DIO mice, their body weight was monitored throughout the 27-week study period. Following the behavioral tests, mice were fasted for 6 h, after which fasting blood glucose was measured from the tail vein using an Elite Glucometer (Bayer, Mishawaka, IN, USA). Serum was also collected via retro-orbital bleeding for the quantification of fasting insulin levels using a mouse-specific enzyme-linked immunosorbent assay (ELISA) kit (JL48252, JONLNBIO, Shanghai, China). A glucose tolerance test (GTT) was then conducted by intraperitoneal injection of a glucose solution (2 g/kg body weight) into mice that had fasted for 6 hours. Blood glucose levels were monitored at 0, 15, 30, 60, 90, and 120 minutes post-injection. Total glycemic excursion was quantified as the area under the curve (AUC) using the trapezoidal rule.

2.3 Behavioral Tests

To assess depressive-like behaviors, all mice underwent a battery of well-validated behavioral tests with a 48-h interval between each test to minimize potential carryover effects. The open field test was conducted to evaluate general locomotor activity and anxiety-like behavior. Each mouse was placed individually in a square arena (50 $\times$ 50 cm) and allowed to explore freely for 5 minutes under dim lighting conditions (20 lux). The number of rearing episodes (upright posture on hind legs) was quantified over the entire 5-minute session. Rearing is a validated measure of exploratory drive and risk-taking behavior, with a reduction in this behavior reflecting a depressive-like anhedonic state and/or heightened anxiety [14]. The number of rearing episodes was quantified over a 5-minute period. The sucrose preference test was performed to measure anhedonia, a core symptom of depression. Mice were first acclimated for 48 h to two bottles, one containing a 1% sucrose solution and the other tap water. Following food and water deprivation for 12 h, mice were individually housed and given free access to both bottles for 4 h [15]. Fluid intake was determined by weighing the bottles before and after the test. To ensure data validity, only mice with a total fluid intake exceeding 0.5 mL during the 4-h test were included in the analysis. All mice in the study met this criterion. Sucrose preference was calculated using the following formula: sucrose preference (%) = [sucrose intake / (sucrose intake + water intake)] $\times$ 100%. The tail suspension test was conducted to assess depression-like behavior. Each mouse was suspended by its tail using adhesive tape attached to a horizontal bar, with its head positioned approximately 30 cm above the surface. The test lasted 6 minutes, and the total duration of immobility during the final 4 minutes was recorded. For the forced swimming test, mice were placed individually into cylindrical containers (height: 25 cm; diameter: 18 cm) filled with water (23–25 °C) to a depth of 15 cm. After a 2-minute acclimatization period, the immobility time was measured over the subsequent 4 minutes. All behavioral sessions were video-recorded and analyzed by experimenters who were blinded to the group assignments.

2.4 Histological Analysis

After the behavioral tests, mice were deeply anesthetized and transcardially perfused with PBS followed by 4% paraformaldehyde (PFA, Shanghai Maokang Biotechnology Co., Ltd, Shanghai, China). The brains were post-fixed overnight at 4 °C and subsequently cryoprotected in 30% sucrose solution. Coronal hippocampal sections (20 µm thick) were prepared using a freezing microtome. For hematoxylin and eosin (H&E) staining, sections were first incubated in H&E solutions (catalog No. K1142, APExBIO, Houston, TX, USA), dehydrated through an alcohol series, and then mounted. For Nissl staining, sections were incubated in Cresyl Violet Stain Solution (1%) (catalog No. ab246817, Abcam, Cambridge, UK), differentiated in alcohol, and a coverslip was added. To assess hippocampal neuronal damage, the number of intact neurons per mm^2 was quantified across three non-overlapping fields in the ventral CA1 subregion. Analyses were performed on sections located between approximately AP –2.9 mm and AP –4.2 mm from Bregma (Paxinos and Franklin's mouse brain atlas), with a representative imaging field centered at AP –3.5 mm, ML $\pm$ 2.5 mm, DV –3.0 mm. Neuronal integrity was assessed using established morphological criteria. Healthy neurons exhibited a large, pale nucleus with a visible nucleolus and abundant Nissl substance. Damaged neurons were identified by characteristic pyknosis (nuclear shrinkage and hyperchromasia) and a marked loss of Nissl bodies (chromatolysis).

2.5 Enzyme-Linked Immunosorbent Assay

Upon completion of the behavioral tests and metabolic phenotyping, mice were deeply anesthetized with sodium pentobarbital (50 mg/kg, i.p.). Blood samples were collected via retro-orbital bleeding. The blood was allowed to clot for 30 min at room temperature and then centrifuged at 3000 $\times$g for 15 min at 4 °C to obtain serum. Subsequently, mice were transcardially perfused with ice-cold PBS, and the brains were rapidly removed. Hippocampi were dissected on a chilled plate, snap-frozen in liquid nitrogen, and stored at –80 °C until analysis. For cytokine analysis, hippocampal tissues were homogenized in cold PBS containing 1$\times$ protease inhibitor cocktail. The homogenates were centrifuged at 12,000 $\times$g for 20 min at 4 °C, and the supernatants were collected. The levels of pro-inflammatory cytokines interleukin-6 (IL-6, PI326, Beyotime, Shanghai, China), interleukin-1β (IL-1β, PI301, Beyotime), and tumor necrosis factor-α (TNF-α, PT512, Beyotime) in hippocampal homogenates and monoamine neurotransmitters (5-HT, NA) in serum were quantified using commercially available ELISA kits, as per the manufacturers' instructions. All samples were analyzed in duplicate, and absorbance was measured at 450 nm using a microplate reader (ELx800, BioTek, Santa Clara, CA, USA).

2.6 Real-Time Fluorescent Quantitative PCR

Total RNA was extracted from samples using TRIzol reagent (catalog No. 15596018CN, Sigma-Aldrich). Complementary DNA (cDNA) was then synthesized from the isolated RNA with a PrimeScript RT reagent kit (catalog No. RR037A, Takara, Kusatsu, Japan). Quantitative real-time PCR (qPCR) was performed on a 7300 Plus Real-Time PCR System (catalog No. JM1966-018481, Thermo Fisher Scientific, Waltham, MA, USA) using SYBR Premix Ex Taq I (Takara, RR820A). The 20 µL reaction mixture contained 1 µL of cDNA template, 10 µL of PCR master mix, 5 pmol of each primer, and nuclease-free water (catalog No. AM9937, Ambion™, Waltham, MA, USA). The PCR protocol involved an initial denaturation at 95 °C for 13 s, followed by 40 cycles of 94 °C for 10 s and 60 °C for 20 s.

Table 1. Primer sequences utilized in this study.

Target gene	Forward primer sequence	Reverse primer sequence
TNF-α	CAGGCGGTGCCTATGTCTC	CCATTTGGGAACTTCTCATCCCTT
iNOS	GGTGAAGGGACTGAGCTGTT	ACGTTCGTTCTCTTGCA
GAPDH	GCCAAGGCTGTGGGCAAGGT	TCTCCAGGCGGCACGCAGA

TNF-α, tumor necrosis factor-α; iNOS, inducible nitric oxide synthase; GAPDH, Glyceraldehyde-3-Phosphate Dehydrogenase.

Gene expression levels were calculated using the comparative ΔΔCt method, with *GAPDH* serving as the internal reference control. All primer sequences are shown in Table 1.

2.7 Isolation of Glial Cell-Enriched Isolates

Glial cell-enriched isolates were obtained from the brains of 16-week-old C57BL/6J mice using a combined enzymatic and mechanical dissociation protocol. In brief, mice were transcardially perfused with ice-cold PBS. The brains were rapidly excised, and the cortices and hippocampi were carefully dissected. The tissues were enzymatically digested in Hank's balanced salt solution (HBSS) (catalog No. 14185052, Thermo Fisher Scientific) supplemented with 2 mg/mL papain (catalog No. LS003126, Worthington, Lakewood, NJ, USA) and 100 U/mL DNase I (catalog No. D5025, Sigma-Aldrich) for 30 minutes at 37 °C. The resulting cell suspension was triturated, filtered through a 70-µm cell strainer, and centrifuged on a 30%/70% Percoll (catalog No. 17089101, GE Healthcare, Chicago, IL, USA) density gradient. Fractions enriched with glial cells were harvested and used as glial cell-enriched isolates from the interphase layer, washed, and subsequently seeded in DMEM/F-12 complete medium for further culture.

2.8 Immunofluorescence Staining

For immunofluorescence staining, brain sections or cultured primary microglia were fixed with 4% PFA, permeabilized with 0.3% Triton X-100 (catalog No. T8787, Sigma-Aldrich), and blocked with 5% bovine serum albumin (BSA, catalog No. A3156-25G, Sigma-Aldrich). Sections or cells were incubated overnight at 4 °C with the following primary antibodies: anti-ionized calcium-binding adapter molecule 1 (Iba1) (1:100, catalog No. ab283319, Abcam) and anti-inducible nitric oxide synthase (iNOS, 1:100, catalog No. ab210823, Abcam), or appropriate combinations for co-staining. Bodipy™ 493/503 (1:600, Thermo Fisher Scientific, Cat. No. D3922) was applied for the detection of LDs. Following three washes with PBS, samples were incubated with Alexa Fluor® 488-conjugated goat anti-rabbit IgG (1:500, A11017, Thermo Fisher Scientific) and Alexa Fluor® 594-conjugated goat anti-mouse IgG (1:500, A-11020, Thermo Fisher Scientific) secondary antibodies for 1 h at room temperature. Nuclei were counterstained with 4',6-diamidino-2-phenylindole (DAPI) (catalog No. D9542-1MG, Sigma-Aldrich). Fluorescent images were acquired using a Nikon A1R HD25 confocal microscope (Nikon Corporation, Tokyo, Japan) equipped with a Plan Apo λ 20x/0.75 NA objective and CFI Plan Apo λ 60x/1.40 NA oil immersion objective. The following laser and filter sets were used: DAPI (excitation 405 nm, emission 450/50 nm), Alexa Fluor 488 (excitation 488 nm, emission 525/50 nm), and Alexa Fluor 594 (excitation 561 nm, emission 595/50 nm). Images were captured at a resolution of 1024 × 1024 pixels. For co-localization analysis, Z-stacks were collected with a 1.0 µm step size, and the pinhole was set to 1 Airy Unit for all channels. To ensure comparability, the imaging settings (laser power, gain, offset) were kept identical for all samples within the same staining batch.

2.9 Oil Red O Staining

Isolated glial cell-enriched isolates were fixed with 4% PFA for 15 minutes and rinsed with PBS. Cells were subsequently incubated with 60% isopropanol (catalog No. 563935, Sigma-Aldrich) for 1 minute to permeabilize the membranes, followed by staining with freshly prepared Oil Red O working solution (catalog No. O0625, Sigma-Aldrich) for 15 minutes at room temperature. After staining, cells were thoroughly washed with distilled water and counterstained with hematoxylin (catalog No. H9627, Sigma-Aldrich) for 1 minute. Brightfield images were captured using a Nikon Eclipse Ni light microscope (ECLIPSE Ni-L, Nikon Corporation). The extent of lipid droplet accumulation was quantified by measuring the integrated optical density (IOD) of Oil Red O staining across five randomly selected fields per sample using ImageJ software (Version 1.41, NIH, Bethesda, MD, USA). ImageJ analysis of immunofluorescence involved automated thresholding ("Analyze Particles") for quantification of the Percent Area/Integrated Density and plugin-based co-localization (Manders' Coefficients), with all analyses performed blinded.

2.10 Flow Cytometric Analysis

For the analysis of apoptosis, glial cell-enriched isolates were stained using the Annexin V-FITC/PI Apoptosis Detection Kit (catalog No. 556547, BD Biosciences, San Jose, CA, USA) as per the manufacturer's instructions. Briefly, cells were resuspended in binding buffer and incubated with Annexin V-FITC (catalog No. 51-65874X,

BD Biosciences) and propidium iodide (PI) for 15 minutes in the dark. The percentage of apoptotic cells was quantified using a BD FACSVerse flow cytometer (catalog No. 651155; BD Biosciences). For the measurement of intracellular reactive oxygen species (ROS), cells were incubated with 10 µM DCFH-DA (catalog No. S0033S, Beyotime Biotechnology, Shanghai, China) at 37 °C for 30 minutes, washed with PBS, and analyzed immediately by flow cytometry. Fluorescence intensity was detected in the FITC channel. All data were analyzed using FlowJo software (BD Biosciences).

2.11 Cell Counting Kit-8 and Lactate dehydrogenase (LDH) Release Assays

To assess the neurotoxic effects of microglia on hippocampal neurons in a transwell co-culture system, neuronal viability and cytotoxicity were evaluated using the CCK-8 and LDH assays, respectively. For the CCK-8 assay, hippocampal neurons were seeded in the lower chamber of 24-well plates. After 24 h of co-culture with microglia in the upper chamber, the CCK-8 reagent (catalog No. CK04, Dojindo Laboratories, Kumamoto, Japan) was added to each well, and the plates were incubated for 2 h at 37 °C. Absorbance was then measured at 450 nm using a microplate reader. Neuronal viability was expressed as a percentage relative to the control group. For the LDH release assay, culture supernatant was collected from the lower chamber after 24 h of co-culture. LDH activity was measured using a Cytotoxicity Detection Kit (catalog No. 11644793001, Roche Diagnostics, Mannheim, Germany) according to the manufacturer's instructions. Absorbance was read at 490 nm. The percentage of LDH release was calculated as follows: (LDH activity in supernatant / total LDH activity) × 100%.

2.12 Transmission Electron Microscopy for Lipid Droplet Observation

Glial cell-enriched isolates were fixed with 2.5% glutaraldehyde (catalog No. G916054-25ml, Macklin, Shanghai, China) overnight at 4 °C and subsequently post-fixed in 1% osmium tetroxide (catalog No. BD9014, Exonlab, Guangzhou, China). Following dehydration through a graded ethanol series, the cells were embedded in EPON resin (catalog No. 02334-500, Polysciences, Warrington, PA, USA). Ultrathin sections (70 nm) were prepared and double-stained with uranyl acetate (catalog No. 22405, Electron Microscopy Sciences, Hatfield, PA, USA) and lead citrate (catalog No. 17800, Electron Microscopy Sciences). The morphology of LDs was examined using a transmission electron microscope (catalog No. HT7800, Hitachi High-Tech Corporation, Tokyo, Japan) at 80 kV. The number and average diameter of LDs were quantified from randomly selected micrographs using ImageJ software.

2.13 Untargeted Lipidomics of Glial Cell-Enriched Isolates

Lipids were extracted from glial cell-enriched isolates using a methyl-tert-butyl ether (MTBE)/methanol-based extraction method. Lipid profiling was carried out using ultra-high-performance liquid chromatography (UHPLC, Waters Corporation, Milford, MA, USA, ACQUITY UPLC I-Class) coupled with tandem mass spectrometry (MS/MS, Thermo Scientific, Q-Exactive HF-X). Chromatographic separation was performed on a C18 column (catalog No. 186005296, Waters Corporation) with a gradient elution program involving acetonitrile and isopropanol. Mass spectrometry data were acquired in both positive and negative ionization modes.

Data processing was conducted using LipidSearch™ software (v4.2) (catalog No. OPTON-30880, Thermo Fisher Scientific) for lipid identification and quantification. Multivariate statistical analyses, including principal component analysis (PCA) and orthogonal partial least squares discriminant analysis (OPLS-DA), were performed using SIMCA-P (v16.0). Significantly altered lipid species were selected based on a variable importance in projection (VIP) value >1.0 and a p-value < 0.05.

3. Results

3.1 High-Fat Diet Induces Characteristic Metabolic Alterations in DIO Mice

HFD induced a significant increase in the body weight of DIO mice, as well as elevated glucose and insulin levels. After 20 weeks of HFD consumption, the body weight of mice in the DIO group was significantly higher than in the control group ($p < 0.001$, Fig. 2A). Furthermore, fasting blood glucose levels in DIO mice were markedly increased compared to controls ($p = 0.001$, Fig. 2B), as well as the fasting insulin levels ($p < 0.001$, Fig. 2C). Following an intraperitoneal glucose challenge, blood glucose levels in DIO mice were substantially higher at all time points measured (0, 15, 30, 60 and 120 minutes), resulting in a markedly elevated glycemic curve (Fig. 2D). Quantitative analysis of the total glycemic response, represented by the AUC, confirmed a significant increase in the DIO group ($p < 0.001$, Fig. 2E). These data clearly indicate the development of glucose intolerance in DIO mice.

3.2 Diet-Induced Obese Mice Exhibit Depressive-like Behaviors and Hippocampal Neuronal Damage

To investigate the impact of diet-induced obesity on depression-related pathology, mice were first subjected to a series of behavioral tests. Compared to the control group, DIO mice exhibited behaviors consistent with depressive-like phenotypes (Fig. 3A). This was evidenced by increased immobility time in both the tail suspension test ($p < 0.001$) and forced swim test ($p < 0.001$), both of which are well-validated paradigms for assessing depression-like behavior. Furthermore, DIO mice exhibited significantly less rear-

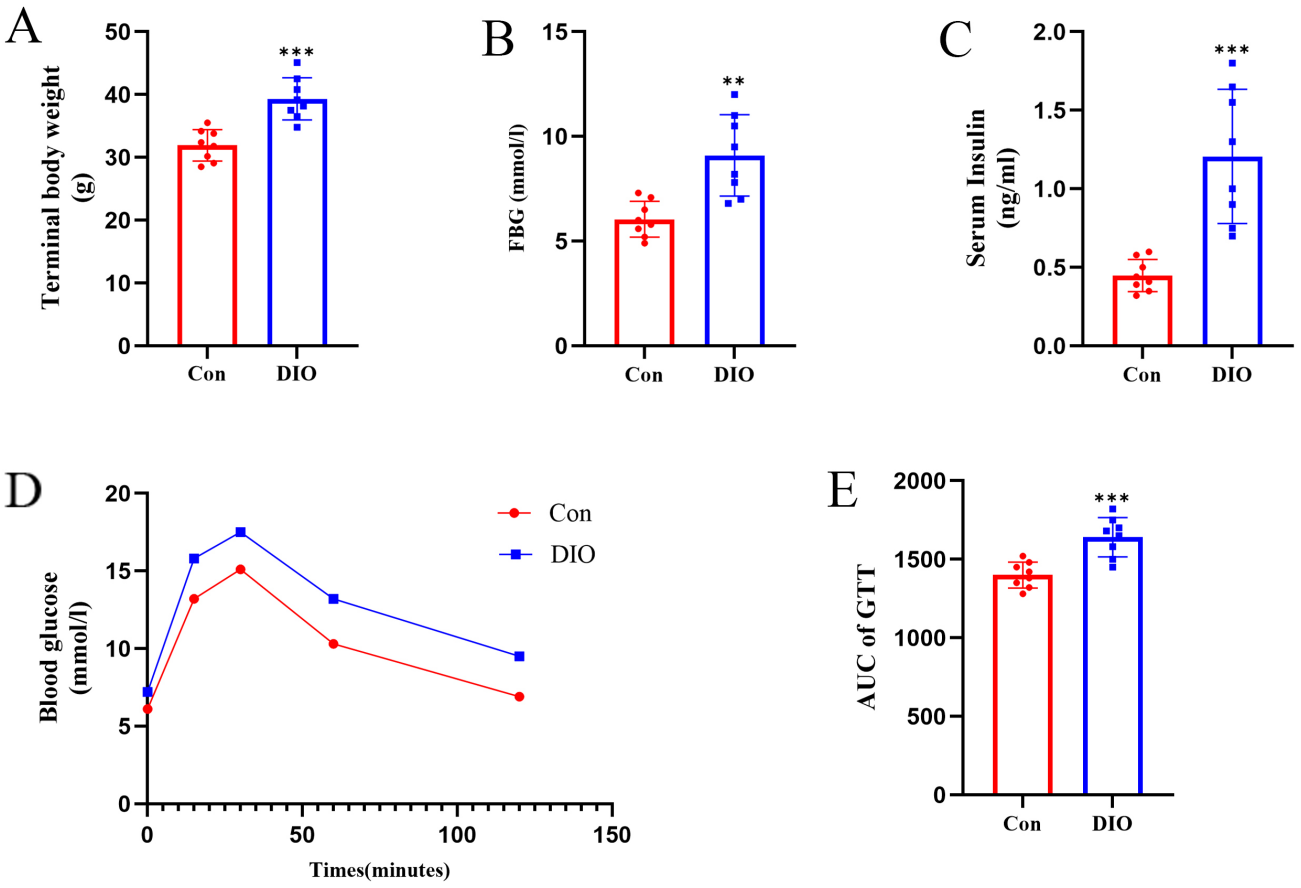

Fig. 2. DIO mice exhibit systemic metabolic dysfunction and glucose intolerance. (A) Terminal body weight of control (Con) and diet-induced obese (DIO) mice after 20 weeks of dietary intervention (n = 8). (B) Fasting blood glucose (FBG) levels (n = 8). (C) Fasting serum insulin concentrations (n = 8). (D) Blood glucose levels during the intraperitoneal glucose tolerance test (GTT) (n = 8). (E) Quantification of the total glycemic response shown as the area under the curve (AUC) for the GTT (n = 8). $^{**}p < 0.005$, $^{***}p < 0.001$.

ing in the open field test ($p = 0.005$), indicating heightened anxiety-like behavior, as well as a significant decrease in sucrose preference ($p < 0.001$), reflecting anhedonia, a core symptom of depression. We next assessed neuronal integrity in the hippocampus, a brain region critically involved in mood regulation. Histological analysis revealed substantial neuronal damage in the hippocampus of DIO mice. Representative images of H&E staining showed marked morphological changes in the DIO group, including pyknotic nuclei (indicated by arrows in Fig. 3B), which are a hallmark of neuronal injury. Quantitative analysis of H&E stained sections confirmed a significant increase in the number of neurons with pyknotic nuclei in DIO mice compared to controls ($p < 0.001$; Fig. 3C). Representative Nissl staining images demonstrated a noticeable reduction in Nissl bodies and a disordered arrangement of neurons in the hippocampus of DIO mice (Fig. 3D). Quantitative analysis of Nissl staining confirmed a significant decrease in the number of healthy Nissl-positive neurons in the DIO group, indicating severe neuronal damage ($p < 0.001$; Fig. 3E). To investigate the potential neurochemical alterations underlying these behavioral and histological deficits, we measured the levels of key monoamine neurotransmitters in the serum. The concentrations of both 5-hydroxytryptamine (5-HT, serotonin; $p = 0.016$; Fig. 3F) and norepinephrine (NA; $p = 0.025$; Fig. 3F) were found to be significantly lower in DIO mice compared to the control group.

3.3 DIO Mice Exhibit Enhanced M1 Polarization and a Pro-inflammatory Profile in Hippocampal Microglia

To determine whether DIO triggers a pro-inflammatory response in the brain, we assessed the polarization state of microglia in the hippocampus. Immunofluorescence double-labeling for Iba1 (a microglial marker) and iNOS (a marker for the M1 pro-inflammatory phenotype) revealed markedly increased co-localization in the hippocampus of DIO mice compared to controls, suggesting a shift towards the M1 polarized state (Fig. 4A). Quantitative analysis confirmed a significant increase in the percentage of iNOS-positive microglia in the DIO group ($p = 0.002$; Fig. 4B). To further validate this pro-inflammatory shift, glial cells from the brains of both groups were iso-

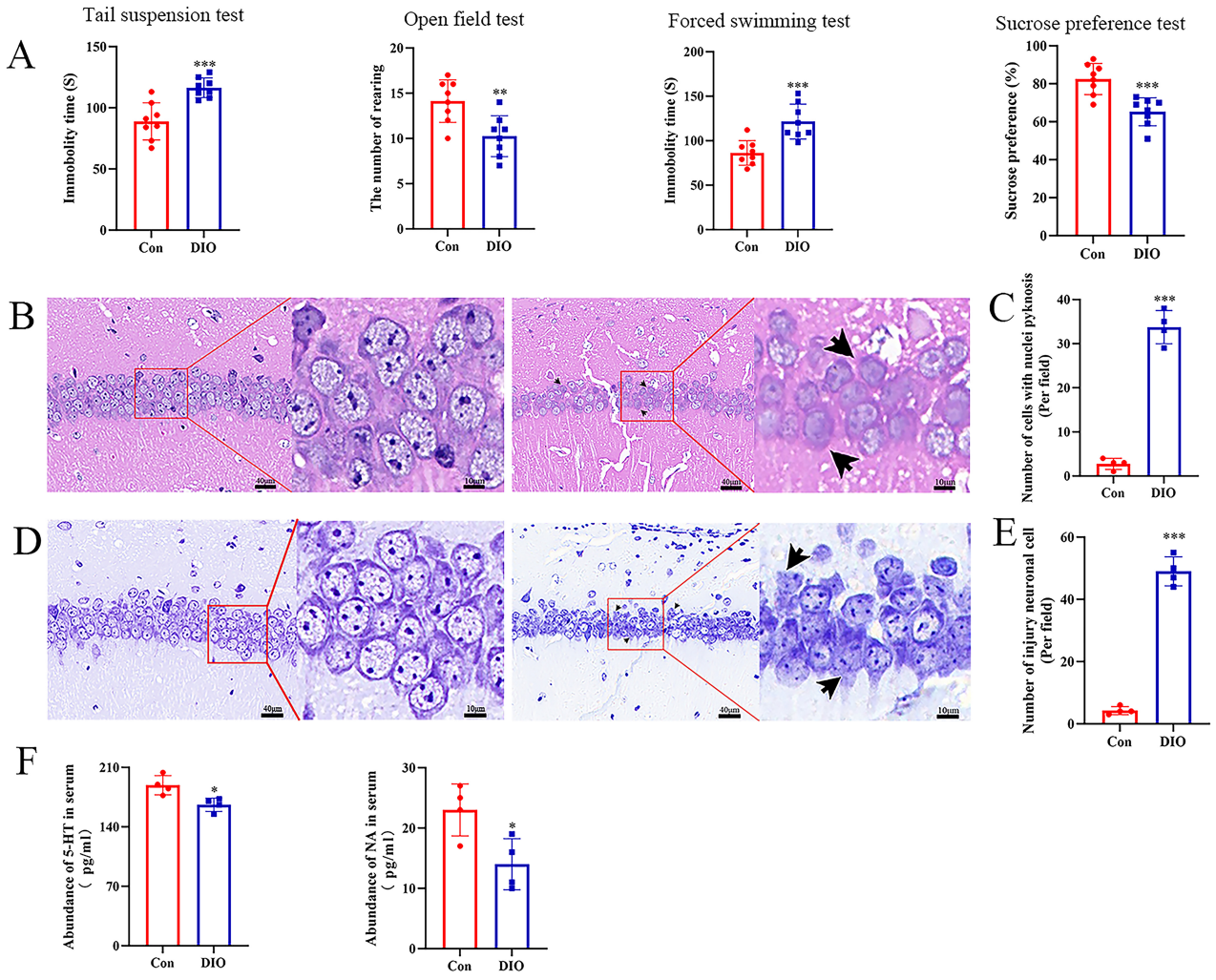

Fig. 3. Depressive-like phenotypes and neuronal damage in DIO mice. (A) Comparison of depressive-like behaviors between groups (n = 8). (B) Representative hematoxylin and eosin (H&E) stained images of the ventral hippocampal CA1 subregion. Pyknotic cells are indicated by black arrows. Scale bars = 40 µm (overview) and 10 µm (inset/enlarged view). (C) Quantification of pyknotic cells in the hippocampus. Damaged neurons are indicated by black arrows (n = 4). (D) Representative Nissl-stained images of the hippocampus. Scale bar = 20 µm. (E) Quantification of hippocampal neuronal damage (n = 4). (F) Abundance of 5-hydroxytryptamine (5-HT) and norepinephrine (NA) in serum (n = 4). *$p < 0.05$, **$p = 0.005$, ***$p < 0.005$.

lated. Representative images of the extracted glial cells are shown in Fig. 4C. Analysis of these cells revealed a significantly enhanced inflammatory profile in the DIO group. At the transcriptional level, mRNA expression of classic M1 markers, including *TNF-α* ($p = 0.008$) and *iNOS* ($p < 0.001$), was significantly upregulated in glial cell-enriched isolates from DIO mice, as measured by qPCR (Fig. 4D). Consistent with the gene expression data, ELISA measurements demonstrated substantially increased secretion of key pro-inflammatory cytokines, namely IL-6 ($p = 0.011$), IL-1β ($p = 0.007$), and TNF-α ($p = 0.002$), in the DIO group compared to the control group (Fig. 4E). Collectively, these results indicate that microglia in DIO mice adopt a pronounced pro-inflammatory state.

3.4 Conditioned Media From DIO Microglia Exerts Neurotoxic Effects on Hippocampal Neurons in a Co-culture System

A transwell co-culture system was established to directly investigate the functional impact of DIO microglia on neuronal health. As schematically illustrated in Fig. 5A, this system allows the exchange of soluble factors between glial cells cultured in the upper chamber and hippocampal neurons cultured in the lower chamber, without direct cell-to-cell contact. We first assessed the viability of hippocampal neurons after exposure to conditioned media from the different microglial populations. The CCK-8 assay revealed the viability of hippocampal neurons co-cultured with DIO microglia was significantly reduced compared to those co-cultured with control microglia ($p =$

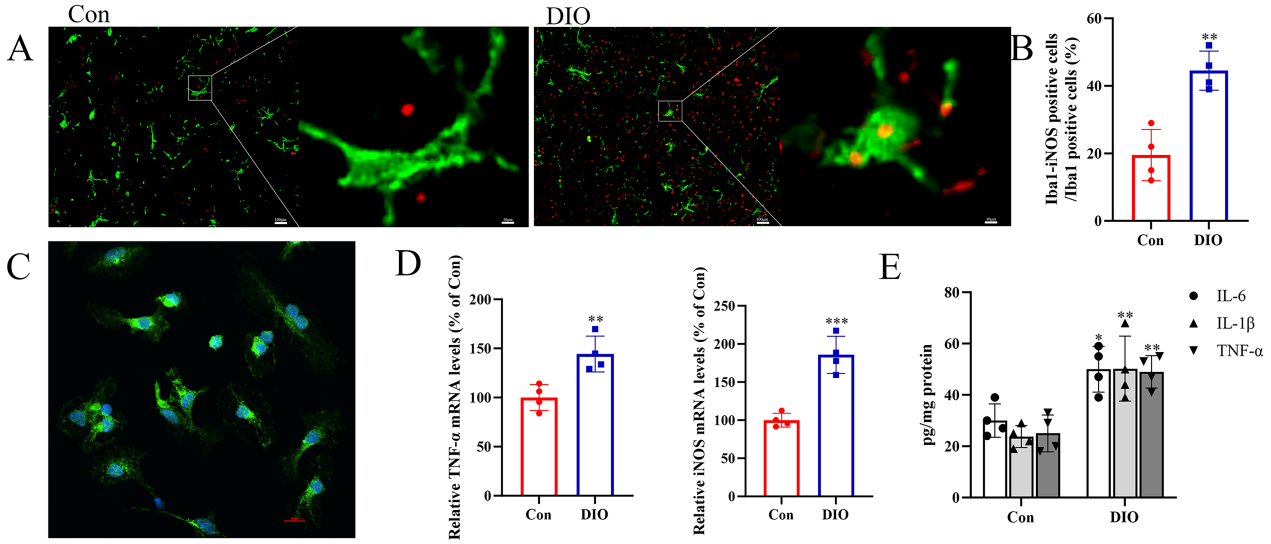

Fig. 4. Hippocampal microglia in DIO mice show enhanced M1 polarization and a pro-inflammatory signature. (A) Representative double immunofluorescence staining of Iba1 and iNOS in hippocampal sections. The white arrow represents an M1-polarized pro-inflammatory microglial phenotype. Scale bars = 100 µm (overview) and 10 µm (inset/enlarged view). (B) Bar chart showing the proportion of double-labeled cells relative to microglia (n = 4). (C) Immunofluorescence of glial cell cultures. Scale bar = 10 µm. (D) mRNA levels of M1 phenotypic markers in glial cells from the two groups (n = 4). (E) Levels of pro-inflammatory cytokines (n = 4). *$p < 0.05$, **$p < 0.01$, ***$p < 0.005$.

0.031; Fig. 5B). Concurrently, the release of LDH, an indicator of neuronal cytotoxicity and membrane damage, was markedly elevated in the co-culture system containing DIO microglia ($p = 0.005$; Fig. 5C). Representative flow cytometry plots (Fig. 5D) and their quantitative analysis confirmed a significantly higher rate of apoptosis in hippocampal neurons exposed to factors derived from DIO microglia ($p = 0.005$; Fig. 5E). Given the established link between inflammation and oxidative stress, we also measured the levels of intracellular ROS. Representative flow cytometry histograms (Fig. 5F) and their quantification revealed a significant increase in ROS accumulation in neurons co-cultured with DIO microglia ($p < 0.001$; Fig. 5G). Taken together, these results demonstrate that soluble factors released by microglia derived from DIO mice can directly induce neurotoxicity, as shown by reduced viability, increased cytotoxicity, elevated apoptosis, and oxidative stress in hippocampal neurons.

3.5 DIO Mice Exhibit Significant Accumulation of Lipid Droplets in Hippocampal Microglia

To investigate the hypothesis that metabolic disturbances in DIO lead to lipid accumulation within microglia, we performed a morphological and ultrastructural analysis. Immunofluorescence staining for Iba1 and Bodipy (a neutral lipid dye) revealed markedly increased co-localization in the hippocampus of DIO mice compared to controls (Fig. 6A), indicating a substantial accumulation of neutral lipids within microglial cells in the DIO group. Quantitative analysis of the fluorescence intensity confirmed a significant increase in Bodipy signal within Iba1-positive cells in DIO mice ($p = 0.015$; Fig. 6B). To further validate these findings at a higher resolution, microglia were examined using transmission electron microscopy (TEM). Representative electron micrographs revealed the presence of large, electron-lucent LDs in the cytoplasm of microglia from DIO mice (Fig. 6C). Taken together, these data provide direct visual and quantitative evidence that DIO induces a state of significant lipid overload, as demonstrated by the accumulation of LDs in hippocampal microglia. Quantitative morphometric analysis of TEM images also revealed a significant increase in the average diameter of LDs within the hippocampal microglia of DIO mice compared to the control group ($p < 0.001$, Fig. 6D). This data provides robust statistical support for the qualitative observation of marked LD accumulation in DIO microglia.

3.6 Glial Cell-Enriched Isolates From DIO Mice Display Enhanced Lipid Accumulation and Triglyceride Content In Vitro

To assess the intrinsic propensity for lipid accumulation in microglia under DIO conditions, we examined primary cells isolated from the DIO and Con groups. Bodipy staining of cultured microglia revealed the presence of LDs (Fig. 7A). Morphometric analysis of these images indicated a distinct pattern of lipid storage: the average size of LDs was significantly larger in microglia from DIO mice ($p = 0.004$; Fig. 7B), whereas the number of LDs per cell was comparable between the two groups ($p = 0.123$; Fig. 7B). This observation was confirmed using an alternative histo-

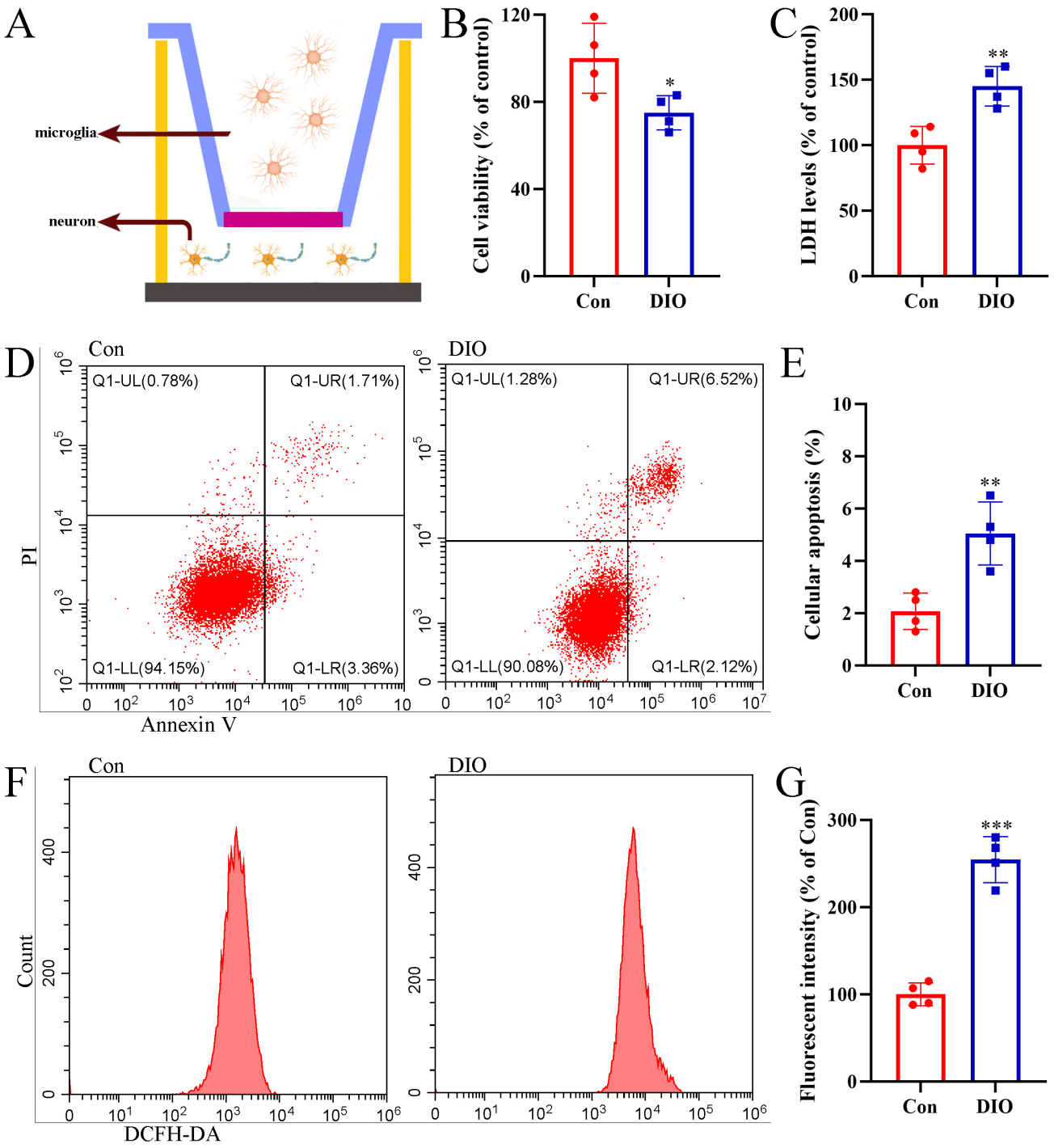

Fig. 5. Neurotoxic effects of DIO microglial conditioned media on hippocampal neurons in a co-culture system. (A) Schematic diagram of a transwell co-culture system. (B) CCK-8 assay results for cell viability (n = 4). (C) Measurement of lactate dehydrogenase (LDH) activity (n = 4). (D) Analysis of apoptosis by flow cytometry. (E) Bar graph showing apoptosis of hippocampal neurons (n = 4). (F) Flow cytometric analysis of intracellular reactive oxygen species (ROS). (G) Bar graph showing the relative fluorescence intensity of ROS (n = 4). *$p < 0.05$, **$p < 0.01$, ***$p < 0.001$.

logical method. Oil Red O staining also demonstrated more substantial lipid accumulation in DIO microglia (Fig. 7C). Densitometric measurement of the staining intensity confirmed a significant increase in total neutral lipid content in the DIO group compared to controls ($p < 0.001$, Fig. 7D). To obtain a biochemical correlate, we also measured intracellular triglyceride levels. This assay demonstrated a significantly higher triglyceride content in glial cells from DIO mice, consistent with the histochemical findings ($p = 0.007$; Fig. 7E). Collectively, these *in vitro* results indicate

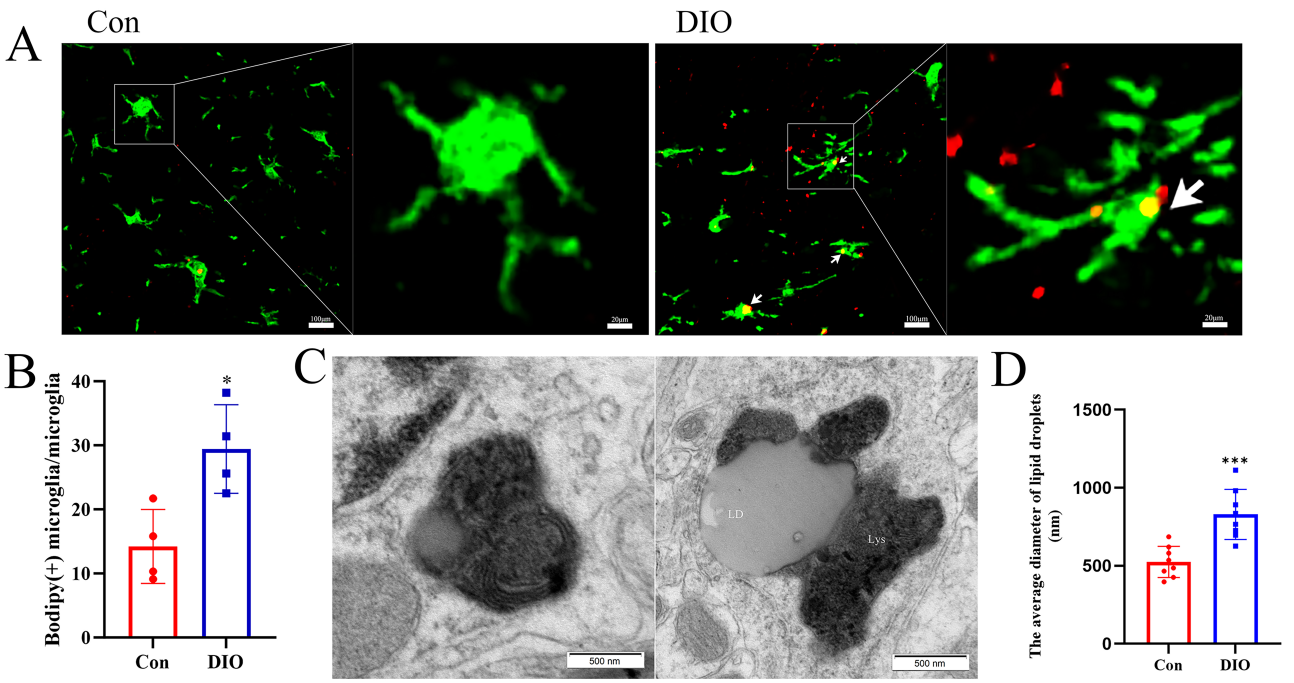

Fig. 6. Lipid droplet accumulation in the hippocampal microglia of DIO mice. (A) Representative immunofluorescence images showing co-localization of Iba1 (green) and Bodipy (red) in the ventral hippocampal CA1 subregion (approximately Bregma –3.5 mm). White arrows indicate lipid droplet-positive microglia. Scale bars = 100 µm (overview) and 20 µm (inset/enlarged view). (B) Proportion of double-stained (Iba1$^+$/Bodipy$^+$) microglia (n = 4). (C) Representative electron micrograph showing lipid droplet size in microglia. Scale bar = 500 nm. LD, lipid droplet; Lys, lysosome. (D) Quantitative analysis of lipid droplet size in microglia (n = 8). *$p < 0.05$, ***$p < 0.001$.

that microglia from DIO mice possess a cell-autonomous predisposition towards excessive lipid storage, characterized primarily by enlarged LDs and increased triglyceride deposition, even in a standardized cell culture environment.

3.7 Lipidomic Profiling Reveals Widespread Alterations in Glial Cell-Enriched Isolates From DIO Mice

To comprehensively investigate the impact of the DIO state on the lipid landscape of microglia, we performed an untargeted lipidomics analysis on glial cells isolated from Con and DIO mice. PCA demonstrated a clear separation between the two groups (Fig. 8A), indicating a distinct global lipidomic profile in DIO microglia. Unsupervised hierarchical clustering of the top 50 most differentially abundant lipids further highlighted pronounced differences, as visualized in a heatmap (Fig. 8B). A ranked metabolite plot detailed these specific alterations (Fig. 8C). Pathway enrichment analyses were performed to gain functional insights. Kyoto Encyclopedia of Genes and Genomes (KEGG) pathway analysis revealed significant enrichment for several lipid metabolism-related pathways, including adipocytokine signaling, fat digestion and absorption, lipid degradation, sphingolipid signaling, glycerophospholipid metabolism, and biosynthesis of unsaturated fatty acids (Fig. 8D). Consistent with these findings, reactome pathway analysis confirmed significant perturbations in key biological processes such as fatty acid transport, sphingolipid metabolism, and overall lipid metabolism (Fig. 8E). Collectively, these data demonstrate substantial and broad rewiring of the lipid metabolic network in the microglia of DIO mice.

4. Discussion

Our study delineates a compelling pathogenic cascade that connects DIO to depression-like pathophysiology, centering on the critical role of hippocampal microglia. The findings suggest that HFD is associated not only with depressive-like behaviors, but also with a profound functional transformation in microglia. This transformation is characterized by the excessive accumulation of intracellular lipid, a phenomenon which in the context of metabolic stress has recently been termed “microglial lipidosis”. The lipid-laden state of microglia is mechanistically linked to a pro-inflammatory, M1-polarized phenotype that drives significant hippocampal neuronal damage. However, it is important to note that the quantitative histological analyses of neuronal damage were conducted with a limited sample size (n = 4 per group). While the observed effects were large, consistent, and supported by our functional co-culture data, future studies with larger cohorts are warranted to confirm

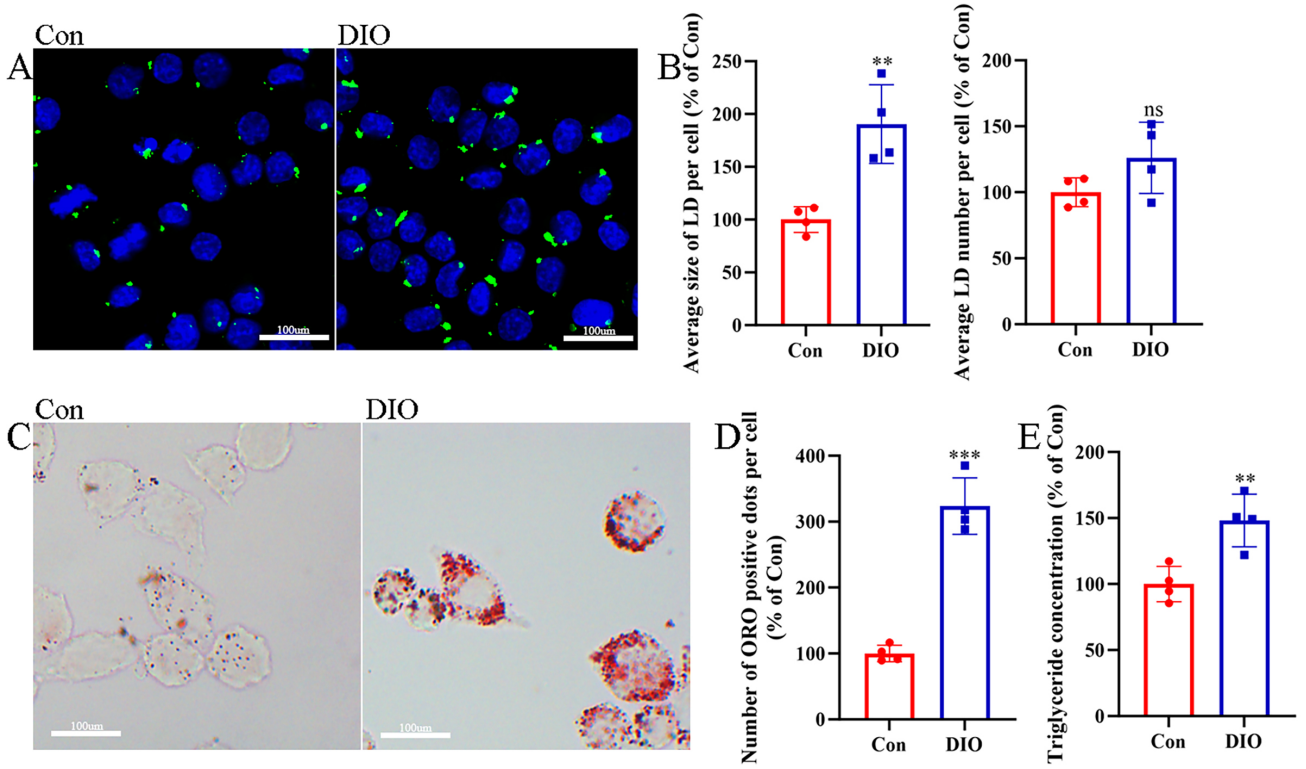

Fig. 7. Enhanced *in vitro* lipid accumulation and triglyceride content in glial cells from DIO mice. (A) Bodipy staining in glial cells. Scale bar = 100 µm. (B) Analysis of lipid droplet size and number in microglia (n = 4). (C) Oil Red O (ORO) staining in glial cells. Scale bar = 100 µm. (D) Normalized number of Oil Red O-positive puncta per cell (n = 4). (E) Normalized intracellular triglyceride (TG) level (n = 4). $^{**}p < 0.01$, $^{***}p < 0.001$, ns, not significant.

these findings. By integrating behavioral, histological, and cellular evidence, our findings position microglial lipid dysregulation as a pivotal mechanism that translates peripheral metabolic distress into inflammation and dysfunction of the central nervous system, thereby expanding the concept of the gut-brain axis in metabolic disorders [16]. Importantly, this pathway identifies several promising avenues for clinical translation, offering new hope for diagnosing and treating the increasingly prevalent condition of metabolic depression.

The transition of microglia from homeostatic sentinels to lipid-laden, pro-inflammatory effector cells appears to be a cornerstone of this process. The pronounced accumulation of LDs, as vividly captured by Bodipy staining and electron microscopy, indicates a state of metabolic overload that overwhelms the normal catabolic functions of these cells. This phenomenon is increasingly recognized in neuroinflammatory conditions such as Alzheimer's disease and other neurodegenerative disorders [17]. Our observations are consistent with recent work showing that metabolic stress can induce a distinct "lipid-droplet-accumulating" microglial state, with impaired phagocytic function and enhanced cytokine production [18,19]. Our lipidomics data confirms the presence of broad alterations in pathways such as glycerophospholipid and sphingolipid metabolism, consistent with prior reports linking lipid dysregulation to neuroinflammation [20,21]. However, the key clinical insights lie not in the specific lipid species that are altered, but in the overarching phenomenon itself. These lipid alterations may contribute directly to the pro-inflammatory phenotype. For instance, lipids enriched with saturated fatty acids could drive the production of pro-inflammatory cytokines (e.g., TNF-α, IL-1β) by activating the toll-like receptor 4/nuclear factor kappa-light-chain-enhancer of activated B cells (TLR4/NF-κB) pathway, which aligns with the cytokine profile we observed in DIO mice. Concurrently, disturbances in sphingolipid metabolism might regulate NLR family pyrin domain containing 3 (NLRP3) inflammasome activity by altering the ceramide-sphingosine-1-phosphate (S1P) balance. The LD-rich microglia in DIO mice represent a tangible, cellular biomarker of pathology. This is highly significant for clinical translation, as it suggests that neuroinflammation in metabolic depression is not an abstract concept, but is in fact associated with a concrete, measurable cellular change. Advanced neuroimaging techniques, such as magnetic resonance spectroscopy (MRS) targeting lipid/glutamine complexes, or the development of specific Positron Emission Tomography (PET) ligands for activated microglia (e.g., Translocator Protein ligands), could potentially be used in human patients to probe this "lipid-laden microglia" phenotype *in vivo*, building on recent advances in neuroinflammation imaging [22,23]. Iden-

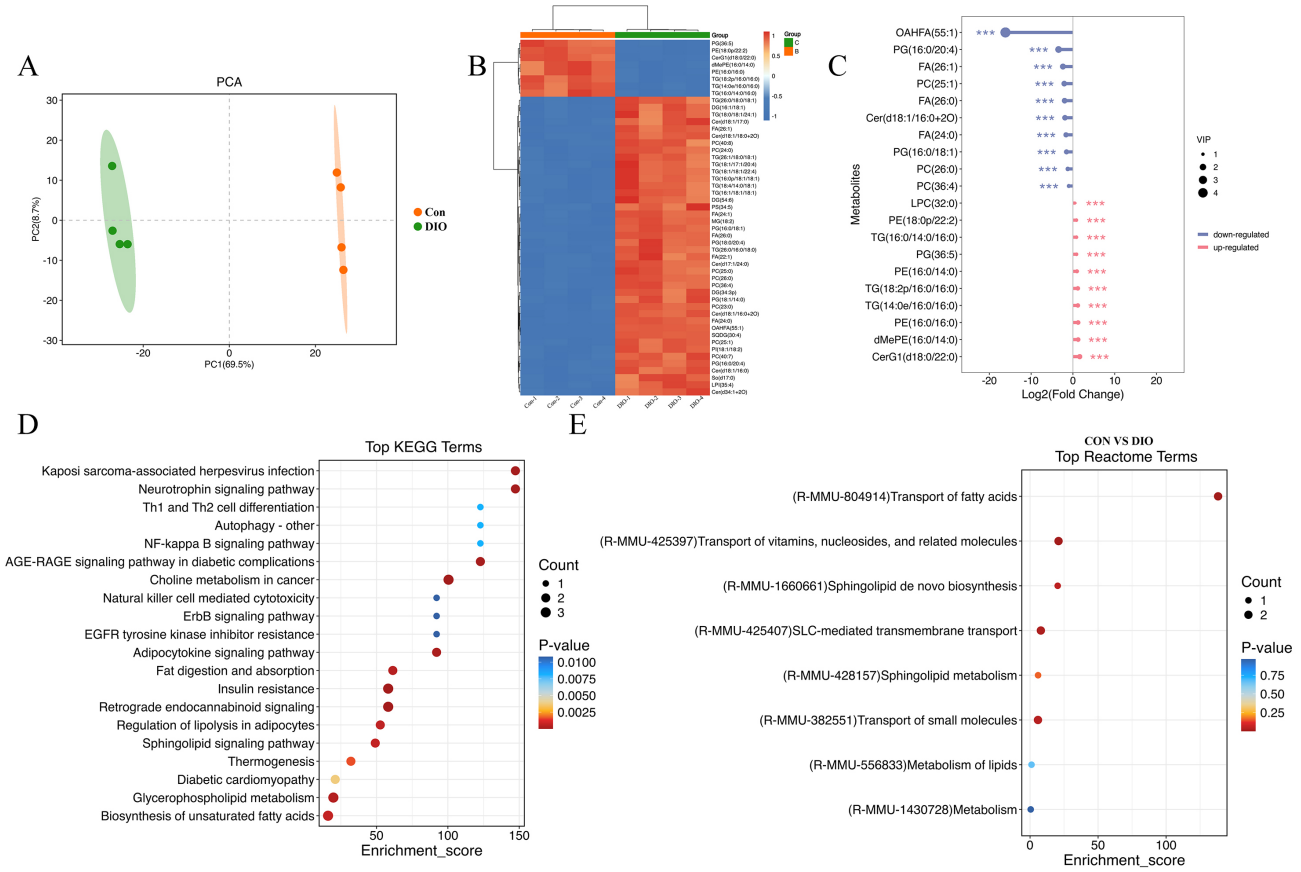

Fig. 8. Lipidomic profiling of glial cells from DIO mice. (A) PCA analysis of untargeted lipidomics. (B) Heatmap analysis of differential metabolites. (C) Visualization of differential metabolites with a lollipop plot. (D) KEGG pathway enrichment analysis. (E) Reactome pathway enrichment analysis. PCA, principal component analysis; KEGG, Kyoto Encyclopedia of Genes and Genomes.

tifying such a biomarker signature could revolutionize patient stratification, allowing clinicians to distinguish a subtype of depression driven primarily by metabolic dysfunction. This subtype may not respond optimally to conventional antidepressants targeting monoaminergic systems, which is consistent with clinical trials showing limited efficacy of Selective Serotonin Reuptake Inhibitors (SSRIs) in patients with metabolic syndrome [24].

Our co-culture experiments established a direct causal link through which glial cell-enriched isolates from DIO mice inflict severe damage on healthy hippocampal neurons. Our findings highlight the therapeutic potential of targeting this microglial dysfunction. The observed neuronal injuries, including increased apoptosis and oxidative stress, provide insight into a potential cellular mechanism that may contribute to hippocampal atrophy and the functional deficits often associated with major depressive disorder [25,26]. Interruption of the deleterious crosstalk from microglia to neurons could therefore represent a rational treatment strategy. The most immediate translational value of our findings may lie in the repurposing of existing metabolic drugs. For instance, peroxisome proliferator-activated receptor agonists, such as the glitazones used in type 2 diabetes, are known regulators of lipid metabolism and possess anti-inflammatory properties. These have shown promise in preclinical models of neuroinflammation [27,28]. Our data provide strong justification for preclinical studies investigating these agents in patients with comorbid obesity and depression, with the rationale being that they could help to normalize lipid metabolism in brain immune cells, thereby reducing neuroinflammation. Similarly, drugs targeting sphingolipid metabolism, another involved pathway in our model, are being developed for other conditions and could also be explored for metabolic depression, given the emerging role of sphingolipids in neurological disease [29,30].

Our work underscores the importance of lifestyle interventions that extend beyond simple weight loss. The fact that a dietary insult can trigger such a dramatic cascade in the brain reinforces the concept that “brain health is metabolic health”, echoing findings from epidemiological studies linking Western-style diets to an increased risk of depression [31,32]. For patients with treatment-resistant depression and metabolic syndrome, structured dietary interventions aimed at reducing systemic inflammation and lipid levels could be prescribed as an adjuvant to psychotherapy or pharmacotherapy, with the specific goal of mitigating the microglial-driven pathway. This provides

a biological rationale for the observed antidepressant effects of anti-inflammatory diets and highlights the need for a more integrated, systemic approach to managing depression, consistent with recent clinical trials demonstrating the efficacy of dietary interventions in depression [33,34].

It is important to acknowledge the inherent limitations of this study. The experimental design utilized male mice only to avoid potential confounders associated with the female estrous cycle. However, this meant we were unable to evaluate sex differences, despite their known importance in human depression and immunometabolism [35,36]. Furthermore, a fundamental question that remains unresolved is whether intervening in microglial lipid metabolism can reverse the pathological process once it has been established. A critical question for future clinical research will therefore be to determine whether lipid accumulation in microglia is a reversible phenomenon. If the sequestration of lipids is an adaptive and protective response to an overwhelming influx, therapeutic strategies that improve systemic metabolism and reduce the lipid burden on the brain may allow microglia to gradually clear their LDs and return to a homeostatic state. This was suggested by a recent study showing metabolic flexibility in microglia [37]. Conversely, if chronic lipid loading leads to an irreversible transformation, then early intervention becomes paramount, emphasizing the need for a preventive approach in individuals with metabolic risk factors. In this case, screening for subclinical depressive symptoms long before the full-blown disorder develops is critical, aligning with recent moves toward precision psychiatry.

Several other limitations of this study should also be acknowledged. First, the sample size for certain analyses was modest, which warrants caution in interpreting the findings. Second, the exclusive use of male mice, while controlling for hormonal variations associated with the estrous cycle, prevents investigation of potential sex differences in the observed effects. These limitations highlight the need for future studies with larger sample sizes and including both sexes to confirm and extend our preliminary observations. Another limitation is the microglial isolation method using Percoll gradient centrifugation. While this method effectively enriches for glial cells, the resulting enriched fraction may also contain other cell types. Thus, the lipidomic alterations reported here, while highly suggestive, were characterized in this enriched fraction rather than in a pure microglial population. Future studies using more stringent purification methods, such as fluorescence-activated cell sorting (FACS) or magnetic-activated cell sorting (MACS), will be essential to confirm the observed changes specifically in microglia.

5. Conclusion

In conclusion, our findings suggest that microglial lipid accumulation and the subsequent neuroinflammatory response may represent a potential mechanistic link between obesity and depression. The primary clinical value of this research is the identification of a novel, druggable pathway that goes beyond the traditional neurocentric view of depression. This shifts the therapeutic focus towards normalizing the metabolic-immune interface within the brain, in line with the growing concept of immunometabolic depression. By reconceptualizing a subset of depression as a disorder of immunometabolism, our findings open the door to more personalized and effective treatment strategies. Targeting lipid metabolism in glial cells, either through novel pharmacologic agents or repurposed metabolic drugs, alongside targeted lifestyle changes, may break the vicious cycle linking poor metabolic health to the devastating experience of depression. This could potentially inform the development of more effective and holistic patient care strategies.

Availability of Data and Materials

The datasets used and analyzed in this study can be obtained from the corresponding author upon reasonable request.

Author Contributions

XJL, JCC, YZX, PZ, and ZP designed the research study. The research and experiments were performed by XJL, ZP, YZX, ZYY, and YLY, with the experimental work primarily conducted by XJL, JCC, YZX, and PZ. XJL and ZP analyzed the data and wrote the manuscript. All authors contributed to editorial revisions, read and approved the final manuscript, and agreed to be accountable for all aspects of the work.

Ethics Approval and Consent to Participate

All animal procedures were performed in accordance with the guidelines approved by the Institutional Review Board of The Affiliated Nanhua Hospital. All animal procedures were approved by the Animal Ethics Committee of Affiliated Nanhua Hospital, University of South China (Approval number: 2025-ky-126). All animal experiments in our study were conducted in strict accordance with National Institutes of Health Guide for the Care and Use of Laboratory Animals.

Acknowledgment

Not applicable.

Funding

This work was supported by Natural Science foundation of Hunan Province (grant number: 2025JJ81092) and the Clinical Medical Technology Innovation Guide Project of Hunan Province, China (grant number: 2021SK51901).

Conflict of Interest

The authors declare no conflict of interest.

Declaration of AI and AI-Assisted Technologies in the Writing Process

During the preparation of this work, the authors used ChatGPT and DeepSeek to assist with language polishing, grammar checking, and formatting suggestions. After using these tools, the authors thoroughly reviewed and revised the content and take full responsibility for the final version of the manuscript.

References

[1] Simon GE, Moise N, Mohr DC. Management of Depression in Adults: A Review. JAMA. 2024; 332: 141–152. https://doi.org/10.1001/jama.2024.5756.

[2] Lof J, Smits K, Melotte V, Kuil LE. The health effect of probiotics on high-fat diet-induced cognitive impairment, depression and anxiety: A cross-species systematic review. Neuroscience and Biobehavioral Reviews. 2022; 136: 104634. https://doi.org/10.1016/j.neubiorev.2022.104634.

[3] Guillemot-Legris O, Muccioli GG. Obesity-Induced Neuroinflammation: Beyond the Hypothalamus. Trends in Neurosciences. 2017; 40: 237–253. https://doi.org/10.1016/j.tins.2017.02.005.

[4] Kocamer Şahin Ş, Aslan E. Inflammation as a Neurobiological Mechanism of Cognitive Impairment in Psychological Stress. Journal of Integrative Neuroscience. 2024; 23: 101. https://doi.org/10.31083/j.jin2305101.

[5] Wang XL, Li L. Microglia Regulate Neuronal Circuits in Homeostatic and High-Fat Diet-Induced Inflammatory Conditions. Frontiers in Cellular Neuroscience. 2021; 15: 722028. https://doi.org/10.3389/fncel.2021.722028.

[6] Marschallinger J, Iram T, Zardeneta M, Lee SE, Lehallier B, Haney MS, *et al*. Lipid-droplet-accumulating microglia represent a dysfunctional and proinflammatory state in the aging brain. Nature Neuroscience. 2020; 23: 194–208. https://doi.org/10.1038/s41593-019-0566-1.

[7] Wei W, Lattau SSJ, Xin W, Pan Y, Tatenhorst L, Zhang L, *et al*. Dynamic Brain Lipid Profiles Modulate Microglial Lipid Droplet Accumulation and Inflammation Under Ischemic Conditions in Mice. Advanced Science (Weinheim, Baden-Wurttemberg, Germany). 2024; 11: e2306863. https://doi.org/10.1002/advs.202306863.

[8] Zareba J, Cattaneo EF, Villani A, Othman A, Streb S, Peri F. NPC1 links cholesterol trafficking to microglial morphology via the gastrosome. Nature Communications. 2024; 15: 8638. https://doi.org/10.1038/s41467-024-52874-6.

[9] Zhang Y, Du B, Zou M, Peng B, Rao Y. Neuronal Ceroid Lipofuscinosis-Concepts, Classification, and Avenues for Therapy. CNS Neuroscience & Therapeutics. 2025; 31: e70261. https://doi.org/10.1111/cns.70261.

[10] Evans AK, Saw NL, Woods CE, Vidano LM, Blumenfeld SE, Lam RK, *et al*. Impact of high-fat diet on cognitive behavior and central and systemic inflammation with aging and sex differences in mice. Brain, Behavior, and Immunity. 2024; 118: 334–354. https://doi.org/10.1016/j.bbi.2024.02.025.

[11] Shi H, Ge X, Ma X, Zheng M, Cui X, Pan W, *et al*. A fiber-deprived diet causes cognitive impairment and hippocampal microglia-mediated synaptic loss through the gut microbiota and metabolites. Microbiome. 2021; 9: 223. https://doi.org/10.1186/s40168-021-01172-0.

[12] Griffin TM, Lopes EBP, Cortassa D, Batushansky A, Jeffries MA, Makosa D, *et al*. Sexually dimorphic metabolic effects of a high fat diet on knee osteoarthritis in mice. Biology of Sex Differences. 2024; 15: 103. https://doi.org/10.1186/s13293-024-00680-6.

[13] Huang B, Wan Q, Li T, Yu L, Du W, Calhoun C, *et al*. Polycationic PAMAM ameliorates obesity-associated chronic inflammation and focal adiposity. Biomaterials. 2023; 293: 121850. https://doi.org/10.1016/j.biomaterials.2022.121850.

[14] Prut L, Belzung C. The open field as a paradigm to measure the effects of drugs on anxiety-like behaviors: a review. European Journal of Pharmacology. 2003; 463: 3–33. https://doi.org/10.1016/s0014-2999(03)01272-x.

[15] Madison CA, Kuempel J, Albrecht GL, Hillbrick L, Jayaraman A, Safe S, *et al*. 3,3'-Diindolylmethane and 1,4-dihydroxy-2-naphthoic acid prevent chronic mild stress induced depressive-like behaviors in female mice. Journal of Affective Disorders. 2022; 309: 201–210. https://doi.org/10.1016/j.jad.2022.04.106.

[16] Carloni S, Rescigno M. The gut-brain vascular axis in neuroinflammation. Seminars in Immunology. 2023; 69: 101802. https://doi.org/10.1016/j.smim.2023.101802.

[17] Jadiya P, Garbincius JF, Elrod JW. Reappraisal of metabolic dysfunction in neurodegeneration: Focus on mitochondrial function and calcium signaling. Acta Neuropathologica Communications. 2021; 9: 124. https://doi.org/10.1186/s40478-021-01224-4.

[18] Haney MS, Pálovics R, Munson CN, Long C, Johansson PK, Yip O, *et al*. APOE4/4 is linked to damaging lipid droplets in Alzheimer's disease microglia. Nature. 2024; 628: 154–161. https://doi.org/10.1038/s41586-024-07185-7.

[19] Gouna G, Klose C, Bosch-Queralt M, Liu L, Gokce O, Schifferer M, *et al*. TREM2-dependent lipid droplet biogenesis in phagocytes is required for remyelination. The Journal of Experimental Medicine. 2021; 218: e20210227. https://doi.org/10.1084/jem.20210227.

[20] Wang A, Wan X, Zhuang P, Jia W, Ao Y, Liu X, *et al*. High fried food consumption impacts anxiety and depression due to lipid metabolism disturbance and neuroinflammation. Proceedings of the National Academy of Sciences of the United States of America. 2023; 120: e2221097120. https://doi.org/10.1073/pnas.2221097120.

[21] Cashikar AG, Toral-Rios D, Timm D, Romero J, Strickland M, Long JM, *et al*. Regulation of astrocyte lipid metabolism and ApoE secretionby the microglial oxysterol, 25-hydroxycholesterol. Journal of Lipid Research. 2023; 64: 100350. https://doi.org/10.1016/j.jlr.2023.100350.

[22] de Los Angeles Gomez M, Serrai H, Bhaduri S, Laleg-Kirati TM. A novel method for Magnetic Resonance Spectroscopy lipid signal suppression using Semi-classical signal analysis and Bidirectional Long short-term memory. Annual International Conference of the IEEE Engineering in Medicine and Biology Society. IEEE Engineering in Medicine and Biology Society. Annual International Conference. 2022; 2022: 317–320. https://doi.org/10.1109/EMBC48229.2022.9871645.

[23] Kim SW, Wiers CE, Tyler R, Shokri-Kojori E, Jang YJ, Zehra A, *et al*. Influence of alcoholism and cholesterol on TSPO binding in brain: PET [^{11}C] PBR28 studies in humans and rodents. Neuropsychopharmacology. 2018; 43: 1832–1839. https://doi.org/10.1038/s41386-018-0085-x.

[24] Beyazyüz M, Albayrak Y, Eğilmez OB, Albayrak N, Beyazyüz E. Relationship between SSRIs and Metabolic Syndrome Abnormalities in Patients with Generalized Anxiety Disorder: A Prospective Study. Psychiatry Investigation. 2013; 10: 148–154. https://doi.org/10.4306/pi.2013.10.2.148.

[25] Xu DH, Du JK, Liu SY, Zhang H, Yang L, Zhu XY, *et al*. Up-regulation of KLK8 contributes to CUMS-induced hippocampal neuronal apoptosis by cleaving NCAM1. Cell Death & Disease. 2023; 14: 278. https://doi.org/10.1038/s41419-023-05800-5.

[26] Dang R, Wang M, Li X, Wang H, Liu L, Wu Q, *et al*. Edaravone ameliorates depressive and anxiety-like behaviors via Sirt1/Nrf2/HO-1/Gpx4 pathway. Journal of Neuroinflammation. 2022; 19: 41. https://doi.org/10.1186/s12974-022-02400-6.

[27] Fang M, Yu Q, Ou J, Lou J, Zhu J, Lin Z. The Neuroprotective Mechanisms of PPAR-γ: Inhibition of Microglia-Mediated Neuroinflammation and Oxidative Stress in a Neonatal Mouse Model of Hypoxic-Ischemic White Matter Injury. CNS Neuroscience & Therapeutics. 2024; 30: e70081. https://doi.org/10.1111/cns.70081.

[28] Yeh JH, Wang KC, Kaizaki A, Lee JW, Wei HC, Tucci MA, *et al*. Pioglitazone Ameliorates Lipopolysaccharide-Induced Behavioral Impairment, Brain Inflammation, White Matter Injury and Mitochondrial Dysfunction in Neonatal Rats. International Journal of Molecular Sciences. 2021; 22: 6306. https://doi.org/10.3390/ijms22126306.

[29] Leal AF, Suarez DA, Echeverri-Peña OY, Albarracín SL, Alméciga-Díaz CJ, Espejo-Mojica ÁJ. Sphingolipids and their role in health and disease in the central nervous system. Advances in Biological Regulation. 2022; 85: 100900. https://doi.org/10.1016/j.jbior.2022.100900.

[30] Phung NV, Rong F, Xia WY, Fan Y, Li XY, Wang SA, *et al*. Nervonic acid and its sphingolipids: Biological functions and potential food applications. Critical Reviews in Food Science and Nutrition. 2024; 64: 8766–8785. https://doi.org/10.1080/10408398.2023.2203753.

[31] Zielińska M, Łuszczki E, Michońska I, Dereń K. The Mediterranean Diet and the Western Diet in Adolescent Depression-Current Reports. Nutrients. 2022; 14: 4390. https://doi.org/10.3390/nu14204390.

[32] Li Y, Lv MR, Wei YJ, Sun L, Zhang JX, Zhang HG, *et al*. Dietary patterns and depression risk: A meta-analysis. Psychiatry Research. 2017; 253: 373–382. https://doi.org/10.1016/j.psychres.2017.04.020.

[33] Firth J, Marx W, Dash S, Carney R, Teasdale SB, Solmi M, *et al*. The Effects of Dietary Improvement on Symptoms of Depression and Anxiety: A Meta-Analysis of Randomized Controlled Trials. Psychosomatic Medicine. 2019; 81: 265–280. https://doi.org/10.1097/PSY.0000000000000673.

[34] Ren M, Zhang H, Qi J, Hu A, Jiang Q, Hou Y, *et al*. An Almond-Based Low Carbohydrate Diet Improves Depression and Glycometabolism in Patients with Type 2 Diabetes through Modulating Gut Microbiota and GLP-1: A Randomized Controlled Trial. Nutrients. 2020; 12: 3036. https://doi.org/10.3390/nu12103036.

[35] Bangasser DA, Cuarenta A. Sex differences in anxiety and depression: circuits and mechanisms. Nature Reviews. Neuroscience. 2021; 22: 674–684. https://doi.org/10.1038/s41583-021-00513-0.

[36] Thomas JT, Thorp JG, Huider F, Grimes PZ, Wang R, Youssef P, *et al*. Sex-stratified genome-wide association meta-analysis of major depressive disorder. Nature Communications. 2025; 16: 7960. https://doi.org/10.1038/s41467-025-63236-1.

[37] Chausse B, Malorny N, Lewen A, Poschet G, Berndt N, Kann O. Metabolic flexibility ensures proper neuronal network function in moderate neuroinflammation. Scientific Reports. 2024; 14: 14405. https://doi.org/10.1038/s41598-024-64872-1.